Chemical Science

ROYAL SOCIETY OF CHEMISTRY

EDGE ARTICLE

View Article Online
View Journal | View Issue

Cite this: *Chem. Sci.*, 2020, **11**, 5494

All publication charges for this article have been paid for by the Royal Society of Chemistry

Received 3rd February 2020
Accepted 29th April 2020

DOI: 10.1039/d0sc00646g

rsc.li/chemical-science

Metal–metal cooperative bond activation by heterobimetallic alkyl, aryl, and acetylide Pt^{II}/Cu^{I} complexes†

Shubham Deolka, [a] Orestes Rivada-Wheelaghan, [a]‡* Sandra L. Aristizábal, [a] Robert R. Fayzullin, [b] Shrinwantu Pal, [c] Kyoko Nozaki, [c] Eugene Khaskin [a] and Julia R. Khusnutdinova [a]*

We report the selective formation of heterobimetallic Pt^{II}/Cu^{I} complexes that demonstrate how facile bond activation processes can be achieved by altering the reactivity of common organoplatinum compounds through their interaction with another metal center. The interaction of the Cu center with the Pt center and with a Pt-bound alkyl group increases the stability of $PtMe_2$ towards undesired rollover cyclometalation. The presence of the Cu^{I} center also enables facile transmetalation from an electron-deficient tetraarylborate $[B(Ar^F)_4]^-$ anion and mild C–H bond cleavage of a terminal alkyne, which was not observed in the absence of an electrophilic Cu center. The DFT study indicates that the Cu center acts as a binding site for the alkyne substrate, while activating its terminal C–H bond.

Introduction

Metal–metal cooperation plays a crucial role in small molecule activation in enzymes and synthetic systems, including homogeneous and heterogeneous catalysts.[1] Many classical catalytic systems rely on the thorough optimization of the ligand environment to induce the desired reactivity at a single metal center. However, there is currently a growing realization that catalysts' reactivities can be significantly altered through close communication with another metal center, either by design or *via* unexpected bimetallic processes, thus enabling new approaches to bond activation.[2]

The second metal may facilitate substrate binding and preactivation or even stabilize the bond activation product (Scheme 1). The adoption of the bimetallic approach has led to many recent advances in stoichiometric and catalytic bond activation processes.[2,3] Bimetallic cooperation is often proposed in many C–C coupling processes, *e.g.* the Cu-to-Pd transmetalation step in the Sonogashira coupling.[4] The accelerating effect of metal additives (*e.g.* Cu salts) in Pd-catalyzed C–C coupling reactions such as Stille and Suzuki coupling is commonly referred to as "the copper effect".[5]

However, a precise understanding of how the reactivity at the single metal center can be affected by communication with a second metal is often lacking due to the synthetic challenges in selective synthesis of such reactive heterobimetallic complexes with a well-defined structure.

While multiple symmetrical ligand platforms have been developed for the construction of homobimetallic complexes,[6] examples of ligand scaffolds that could selectively support metal–metal interactions between two different metals and at the same time contain available reactive sites, are exceedingly rare.[7] This is especially the case when the combination of a 1st row and a late 2nd or 3rd row transition metal is targeted. Among known heterobimetallic complexes, rigid ligand design often blocks access to coordination sites suitable for cooperative

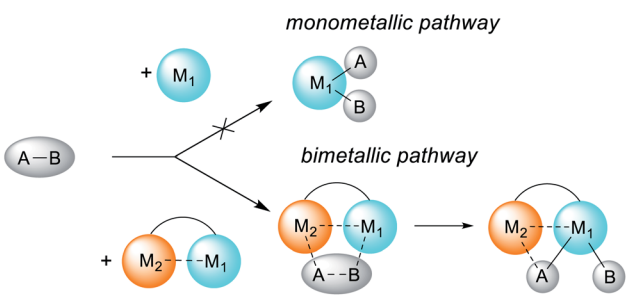

Scheme 1 Schematic representation of the altering reactivity of a single metal center through heterobimetallic complex formation.

[a]*Coordination Chemistry and Catalysis Unit, Okinawa Institute of Science and Technology Graduate University, 1919-1 Tancha, Onna-son, 904-0495, Okinawa, Japan. E-mail: juliak@oist.jp; orestes.rivada@u-paris.fr*

[b]*Arbuzov Institute of Organic and Physical Chemistry, FRC Kazan Scientific Center, Russian Academy of Sciences, 8 Arbuzov Street, Kazan, 420088, Russian Federation*

[c]*Department of Chemistry and Biotechnology, Graduate School of Engineering, The University of Tokyo, 7-3-1 Hongo, Bunkyo-ku, Tokyo 113-8656, Japan*

† Electronic supplementary information (ESI) available. CCDC 1975187–1975194. For ESI and crystallographic data in CIF or other electronic format see DOI: 10.1039/d0sc00646g

‡ Current address: Orestes Rivada-Wheelaghan: Université de Paris, Laboratoire d'Electrochimie Moléculaire, UMR 7591 CNRS, 15 rue Jean-Antoine de Baïf, F-75205 Paris Cedex 13, France.

substrate binding.[8] Although several other classes of binucleating bridging ligands have been developed, many of these ligands do not allow for close metal–metal interactions in homo- or heteropolymetallic systems.[9]

In this work, we report a new bifunctional soft/hard unsymmetrical ligand scaffold, which selectively incorporates both Pt^{II} and Cu^{I} centers. The close proximity between the two metals allows for coordination of alkyl, aryl, or acetylide ligands to both metal centers, and for the dialkyl complexes, enables metal–metal interaction. These heterobimetallic complexes allow us to directly observe the effect of the second metal center on the reactivity of Pt, which is interesting given that Pt complexes with d^{10} metal additives are widely used in C–H bond activation[10] and studied as models for Pd-catalyzed cross-coupling.[11] Our findings demonstrate that even subtle interactions between two different metals alter the solution reactivity of common organometallic species, particularly in the C–H bond activation and boron-to-metal transmetalation reactions, and ligand architecture that induces proximity significantly affects reactivity.

Results and discussion

Ligand design and synthesis of monometallic and heterobimetallic complexes

We have previously reported the reversible stepwise formation of homomultimetallic Cu^{I} linear chain complexes using an unsymmetrical napthyridinone-based ligand $\mathbf{L_0}$ (Scheme 2).[12] Simple functionalization of the O-atom of this ligand by reaction with chlorobis(*tert*-butyl)phosphine leads to a new ligand **L**, in which two well-defined coordination sites are created: a hard-donor site containing a picolylamine arm and a soft-donor site containing a phosphinite arm. We first tested if ligand **L** shows differentiation between soft and hard Lewis acids using $(NBD)Pt^{II}Me_2$ (NBD = norbornadiene) and $[Pt^{IV}Me_3I]_4$ precursors, respectively. As expected, the specific binding of the Pt^{II} center to the soft phosphinite site only is observed, giving complex **1**. The Pt^{IV} center, on the other hand, specifically binds to the hard N-donor site (complex **2**). Interestingly, upon reacting complex **1** with methyl iodide, immediate migration of the Pt center from the soft to the hard site is observed, presenting an alternative pathway for the formation of **2**. The mono-metallic reactivity thus confirms a proof-of-concept for using this ligand platform further in designing heterobimetallic systems selectively *via* the soft/hard Lewis acid concept.

Next we targeted the formation of heterobimetallic complexes using Pt^{II} and Cu^{I} precursors as this combination is known to show metallophilic closed-shell d^8–d^{10} interactions.[13] First, treatment of complex **1** with 2 equiv. of $Cu^{I}Cl$ led to the formation of the heterobimetallic $Pt^{II}Me_2/Cu^{I}$ complex $\mathbf{3}[Cu^{I}Cl_2]$ (Scheme 3). By comparison, the reaction with 1 equiv. of $Cu^{I}Cl$ gave a mixture of products with the major species characterized by an ^1H NMR spectrum similar to that of complex $\mathbf{3}[Cu^{I}Cl_2]$ indicative of the formation of a similar Cu^{I}/Pt^{II} core; however, the reaction was generally less clean and did not proceed with high yield. To avoid the presence of a potentially non-innocent counter anion, $[Cu^{I}(MeCN)_4][X]$ (X = BF_4 or $B(Ar^F)_4$; $B(Ar^F)_4$ = tetrakis[3,5-bis(trifluoromethyl)phenyl]borate) was used leading to complexes $\mathbf{3}[BF_4]$ and $\mathbf{3}[B(Ar^F)_4]$, respectively.

All complexes were isolated in 65–71% yields, characterized by X-ray diffraction (XRD) (*vide infra*), NMR, IR, and UV-vis spectroscopies, ESI-MS, and elemental analysis.

Noting that the ligand platform also contains an acidic benzylic CH_2 position and the previously reported ability of the mononucleating PNN pincer ligands to undergo an N-bound CH_2-arm deprotonation coupled with dearomatization,[14] we attempted the dearomatization of our binucleating P,N-donor ligand **L** using a strong base.

Gratifyingly, treatment of $\mathbf{3}[CuCl_2]$ with KO^{t}Bu resulted in a deep red solution, from which **4** could be isolated cleanly. Complex **4** features a dearomatized naphthyridine ring owing to the deprotonation of its CH_2 arm and thus is the first example of a dearomatized heterobimetallic complex, resembling dearomatization in pincer-based mononucleating ligands utilized for metal–ligand cooperation catalysis.[15] Dearomatization of the naphthyridine-based binucleating PNNP ("expanded pincer") ligand has also been recently reported by Broere and co-workers in a homobimetallic Cu_2 complex.[6f]

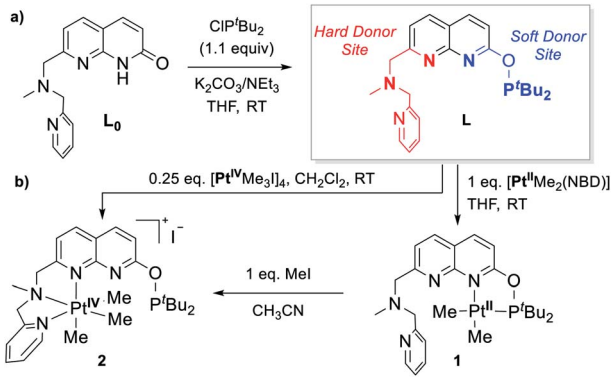

Scheme 2 (a) Synthesis of ligand L; (b) selective binding to Pt^{II} and Pt^{IV} centers *via* hard and soft sites.

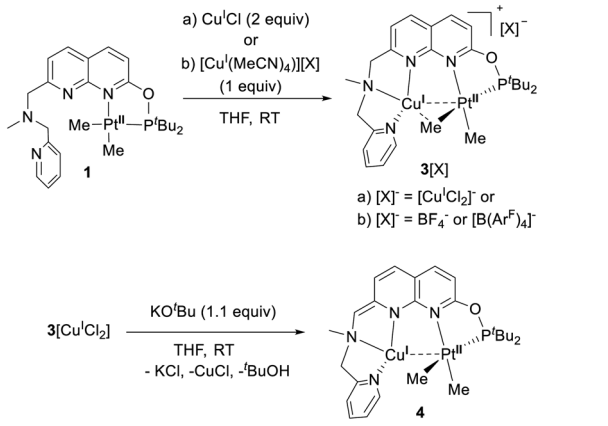

Scheme 3 Formation of cationic heterobimetallic complexes 3[X] and a dearomatized heterobimetallic complex 4.

Characterization of heterobimetallic complexes in the solid state and solution and analysis of metal–metal interactions

The structures of complexes **3**[X] and **4** were confirmed by single crystal XRD studies (Fig. 1).[16] The geometries of the Pt centers in **3**[X] are distorted square planar, with τ_4 and τ_4' values[17] in the range of 0.10–0.13 and 0.07–0.09, respectively (the value for ideal square planar geometry is 0). This indicates that the oxidation state of the Pt center is unlikely to change upon the formation of a heterobimetallic species and it can be formally assigned as +2, consistent with solution NMR studies (*vide infra*). The $Pt^{II}\cdots Cu^{I}$ distances (2.6119(3)–2.6486(3) Å) are shorter than the sum of covalent radii (2.68 Å),[18] but slightly longer than in the $Pt^{II}Me_2/Cu^{I}$ complex reported by Chen *et al.* (2.5275(7) Å).[11] Interestingly, Cu^{I} in **3**[X] has close interaction with the carbon of the proximal Me group with Cu1⋯C1 distances of 2.160(3)–2.362(9) Å. Thus, complexes **3**[X] are the examples of a solution-stable heterobimetallic complex with an unsymmetrical bridging Me group.[19]

Interestingly, the dearomatized complex **4**, characterized by three molecules in the asymmetric cell, features a noticeably longer interaction between Cu^{I} and Pt^{II}, 2.6890(5)–2.7459(6) Å, which is not much larger than the sum of the covalent radii.[18] The distances from C of the proximal Me group to Cu^{I} are longer (2.518(5)–2.559(5) Å) compared to that of complexes **3**[X]. These structural changes are ascribed to the loss of electrophilicity at a formally neutral Cu^{I} center in **4** leading to weakening interactions of Cu^{I} with both Pt^{II} and the bridging Me group. The selected interatomic and bond distances in complexes **3**[X] and **4** and the τ_4 and τ_4' values[17] for the Pt centers are summarized in Tables 1 and 2. The comparison between complexes **3**[X] and **4** shows that the distances between Pt and the carbon of the bridging Me group are consistently longer in complexes **3**[X] demonstrating stronger interaction of the bridging Me group with the Cu^{I} center as compared to **4**. Dearomatization of the ligand in **4** is evident from X-ray diffraction data featuring double bond character (1.359(6)–1.371(7) Å) in the deprotonated arms as opposed to C11–C12 of 1.512(3) Å in the non-dearomatized complex **3**[$CuCl_2$].

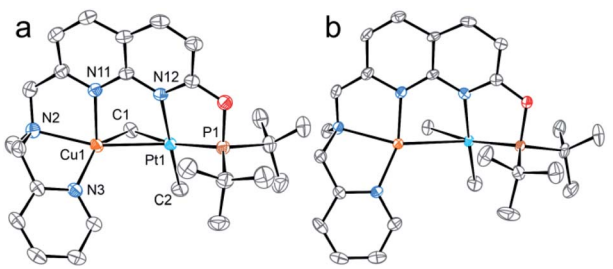

Fig. 1 ORTEP of **3**[$B(Ar^F)_4$] (a) and **4** (b) at the 50% probability level. Hydrogen atoms, the counterions for **3**[$B(Ar^F)_4$], and solvent molecules for **4** are omitted for clarity. In the case of **4**, only one of three symmetrically independent molecules is shown. Hereinafter coordination bonds are shown in accordance with AIM analysis for the gas-phase optimized structures.

Table 1 Selected interatomic and bond distances in complexes **3**[X] determined by XRD and τ_4 values for the Pt center

Bond distance[a] (Å)	**3**[$CuCl_2$]	**3**[BF_4]	**3**[$B(Ar^F)_4$]
Pt1–C1	2.201(2)	2.251(12)	2.164(3)
Pt1–C2	2.050(2)	2.048(11)	2.048(3)
Pt1–N12	2.1823(19)	2.172(9)	2.1894(19)
Pt1–P1	2.2280(6)	2.228(3)	2.2180(6)
Cu1–N11	2.064(2)	2.038(10)	2.076(2)
Cu1–N2	2.320(2)	2.335(11)	2.322(2)
Cu1–N3	1.966(2)	1.982(10)	1.953(2)
Cu1–C1	2.277(2)	2.362(9)	2.160(3)
Pt1–Cu1	2.6486(3)	2.625(2)	2.6119(3)
τ_4	0.10	0.10	0.13
τ_4'	0.07	0.07	0.09

[a] Atom numbering is according to Fig. 1a.

ESI-MS analysis also confirmed that the bimetallic cationic Pt^{II}/Cu^{I} species $\mathbf{3}^{+}$ is present in polar solvents (MeCN or THF), confirming its stability.

NMR spectra of complexes **3**[BF_4] and **3**[$B(Ar^F)_4$] exhibit well-resolved, sharp proton resonances. Diagnostic features of the NMR spectra corresponding to the proximity of a Cu^{I} center to the Pt–Me group in **3**[X] (X = BF_4 and $B(Ar^F)_4$) are compared to those of **1** and **4** in Tables 3 and S1.† The position of the Me groups was determined by selective nuclear Overhauser effect (NOE) experiments. The Me_A group located between the Pt^{II} and Cu^{I} atoms shows a significant downfield shift of the ^{13}C signal by *ca.* 21 ppm compared to the analogous Me_A group located *trans* to the phosphinite in the Cu-free analogue **1**. In

Table 2 Selected interatomic and bond distances in complex **4** determined by XRD and τ_4 values for the Pt center[a]

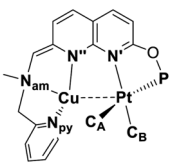

Bond distance[b] (Å)	**4**[c]	**4**[d]	**4**[e]
Pt–C_A	2.109(5)	2.127(5)	2.124(5)
Pt–C_B	2.062(5)	2.050(5)	2.060(5)
Pt–N′	2.156(3)	2.174(4)	2.171(3)
Pt–P	2.2371(11)	2.2428(11)	2.2427(11)
Cu–N″	1.933(4)	1.939(4)	1.939(4)
Cu–N_{am}	2.346(4)	2.317(4)	2.301(4)
Cu–N_{py}	1.925(4)	1.937(4)	1.941(4)
Cu–C_A	2.558(5)	2.518(5)	2.559(5)
Pt–Cu	2.6890(5)	2.7459(6)	2.7201(5)
τ_4	0.12	0.10	0.11
τ_4'	0.07	0.07	0.07

[a] For each symmetrically independent molecule. [b] General scheme for atom labelling in coordination spheres of Pt and Cu is shown above. [c] From XRD data for the 1st symmetrically independent molecule. [d] From XRD data for the 2nd symmetrically independent molecule. [e] From XRD data for the 3rd symmetrically independent molecule.

Table 3 Diagnostic chemical shifts and coupling constants of complexes **1**, **3**[X] and **4** in THF-d_8

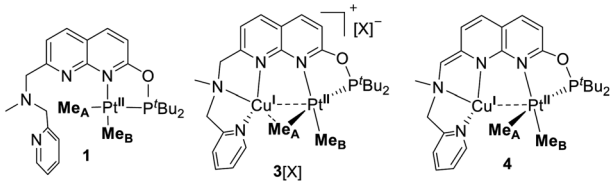

	δ_H ($^2J_{H,Pt}$, Hz)		δ_C ($^1J_{C,Pt}$, Hz)		δ_{Pt} ($^1J_{P,Pt}$, Hz)
Complex	Me_A	Me_B	Me_A	Me_B	Pt
1	0.93 (66)	0.96 (94)	15.7 (662)	−21.9 (805)	−3894 (2006)
3[$B(Ar^F)_4$]	1.10 (44)	1.23 (86)	−5.9 (491)	−21.3 (711)	−3971 (2877)
3[BF_4]	1.04 (36)	1.18 (82)	−5.6 (n.d.)[a]	−21.3 (719)	−3971 (2866)
4	0.82 (56)	0.88 (84)	3.0 (n.d.)[b]	−20.2 (n.d.)[b]	−3980 (2467)

[a] Not determined due to low intensity caused by insufficient solubility; the corresponding $^1J_{C,Pt}$ for Me_A in CD_3CN solution was determined to be 505 Hz (see Table S1). [b] Not determined due to low intensity caused by insufficient solubility.

comparison, almost no change in chemical shift was observed for the Me_B group distal from the Cu^I center of **3** as compared to **1**. The latter observation is also consistent with a Pt^{II} formal oxidation state assignment in complexes **3**[X] and **4** despite the presence of metal–metal interactions. This is also in line with the previous studies by Chen and co-workers who described d^8–d^{10} interactions between an electron-rich Pt^{II} center and a Lewis acidic d^{10} metal, which have a significant donor–acceptor character and are described as Pt→M dative bonds.[13] Moreover, considerably smaller Pt–H and Pt–C coupling constants were observed for the Me_A group of complexes **3**[X] compared to **1**, while only minor changes are seen in the distal Me_B. As expected from crystallographic data, neutral complex **4** features a Me_A group with the ^{13}C chemical shift and coupling constant values that are intermediate between those observed for complexes **3**[X] and **1**, consistent with a weaker Cu/Pt–Me interaction when compared to **3**[X]. Coordination of the Cu^I center also leads to an upfield shift of the ^{195}Pt signal, which shows a larger coupling constant to the P-atom when short $Pt^{II}\cdots Cu^I$ contacts are present. At the same time, ^{195}Pt chemical shifts for complexes **1**, **3**[X] and **4** are significantly upfield shifted as compared to the characterized Pt^{IV} complex **2** (δ_{Pt} −2320.9) supporting the assigned formal Pt^{II} oxidation state in these complexes and consistent with the earlier literature reports.[20]

Dearomatization of the naphthyridine ring in complex **4** was also observed in the ^1H NMR spectrum, showing a significant upfield shift for the naphthyridine protons compared to **3**[X] and **1** (Fig. 2 and S77†), and the presence of a CH group singlet at 4.83 ppm in THF-d_8 solution.

Atoms in Molecules (AIM) analyses for DFT-optimized structures of complexes **3** and **4** revealed that bond critical points (bcp) were located between Pt and Cu atoms (Fig. 3) with characteristics typical for closed-shell, metal–metal interactions (positive value for $\nabla^2\rho_b$, low ρ_b, negative V_b and H_b, with H_b value close to zero).[21] Interestingly, the bcp was also located between Cu and carbon of the proximal Me_A group in complex **3** with characteristics indicative of metal–ligand interactions (ρ_b 0.059 a.u.; $\nabla^2\rho_b$ 0.218 a.u.), but not in complex **4**, consistent with longer Cu⋯C distances observed by XRD. The characteristics for the bond critical points for all complexes are listed in Tables S2–S5 in the ESI.† The comparison between bond distances obtained in the geometry-optimized structures used for QTAIM analysis and XRD parameters show reasonable agreement and the expected trend in $Pt^{II}\cdots Cu^I$ and $Cu^I\cdots Me_A$ contacts (Tables S6–S9†), showing longer $Pt^{II}\cdots Cu^I$ and $Cu^I\cdots Me_A$ distances in complex **4** as compared to **3**.

NBO analysis also shows that complex **3** exhibits strong electron density donation from the proximal Pt–Me_A fragment to an *s*-type orbital on Cu [$\sigma(Pt–C_A(sp^3)\rightarrow Cu(s))$; $E^{(2)}$ = 89.68 kcal mol^{-1}] (Table S11 and Fig. S153†). The metal–metal interactions are manifested in a moderate donation from a d-type orbital on the Pt center to an s-orbital on Cu [Pt(d)→

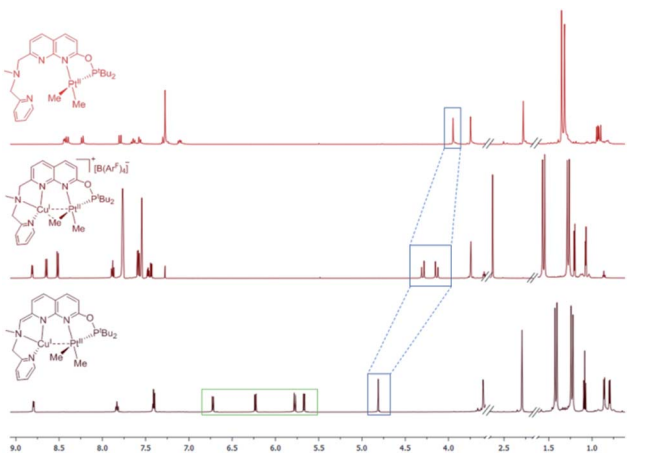

Fig. 2 ^1H NMR spectra (THF-d_8, 25 °C) of isolated complexes **1** (top), **3**[$B(Ar^F)_4$] (middle) and dearomatized complex **4** (bottom). Blue rectangles highlight the naphthyridine-CH_2 signal or *CH* for **4**. Green rectangle highlights the naphthyridine C_{sp^2}–*H* signals of **4**.

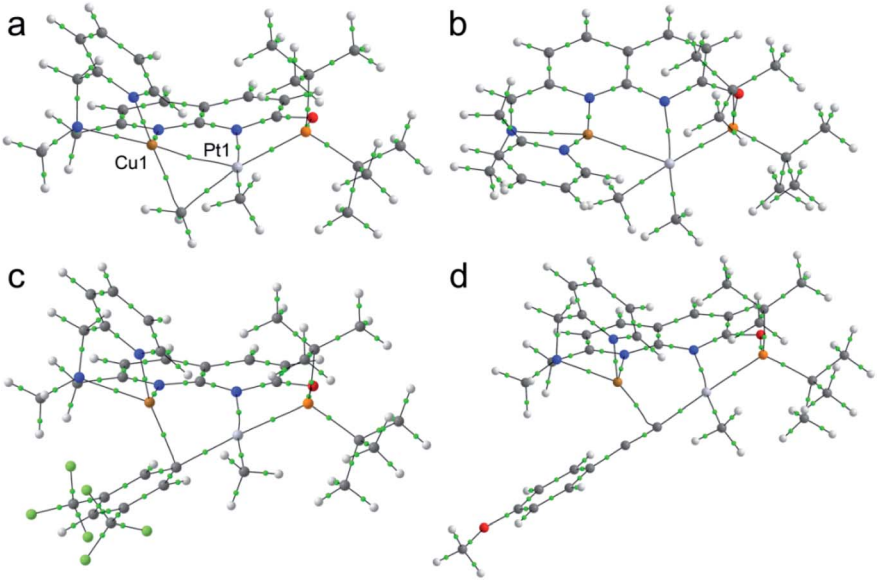

Fig. 3 Molecular graphs for "gas-phase" DFT-optimized complexes 3^+ (a), **4** (b), 6^+ (c), and 7^+ (d). Bond critical points (3, −1) with a threshold of $\nabla\rho_b > 0.025$ a.u. and corresponding bond paths are shown with green dots and black lines, respectively.

Cu(s); $E^{(2)} = 24.49$ kcal mol^{-1}]. Interestingly, the distal Pt–Me_B fragment also shows a donation to a Cu center [σ(Pt–$C_B(sp^3)$→Cu(s)); $E^{(2)} = 25.67$ kcal mol^{-1}], albeit much weaker compared to the donation from Pt–Me_A. A weak back-donation is also found from the d-type orbitals on Cu to a Pt–Me_A [$E^{(2)}$ = 6.0 kcal mol^{-1}] and a Pt–Me_B fragments [$E^{(2)} = 3.0$ kcal mol^{-1}].

The predominant interaction of the proximal Pt–Me_A fragment with a Cu center is also evident from the comparison of the Natural Binding Index (NBI): an NBI between Cu and a carbon atom of Me_A is 0.3476, as compared to a much lower NBI between Cu and a carbon atom of Me_B (0.0946) (Table S12†). The Pt→Cu interaction results in an NBI of 0.2687 between the Pt and Cu centers. The comparison of complex **3** and copper-free complex **1** shows a strong effect of the coordination of the Cu center with a bridging Me_A ligand resulting in the elongation of the Pt–Me_A bond from 2.08 Å in **1** to 2.15 Å in **3**. At the same time, the Pt–Me_B bond length remains essentially unchanged (at 2.05 Å) in both complexes, showing that the effect of Cu on the Pt–Me_B bond length is negligible. Accordingly, the NBI between Pt–Me_A is noticeably lower in complex **3** (0.6760) compared to complex **1** (0.7444), while only minor changes are seen in the NBI for the Pt–Me_B fragment (0.8403 and 0.8301 in complexes **3** and **1**, respectively) (Tables S10 and S12†).

This analysis confirms that the three-center two-electron binding in complex **3** can be best described as a donor–acceptor interaction between a bridging Pt–Me_A and the Lewis-acidic Cu center that is further supported by the Pt→Cu interaction. The distance between Cu and carbon of the Me_A fragment remains significantly longer (Tables 1 and S6†) compared to that in the symmetrical Me-bridged dicopper complex with a naphthyridine-based ligand reported by Tilley and co-workers (2.06–2.08 Å), which showed a three-center, two-electron bond with essentially equivalent binding of the bridging Me to both Cu centers.[22] The donor–acceptor type σ(Pt–Me_A)→Cu(s) three-center, two-electron interaction in **3** is perhaps unsurprisingly unsymmetrical due to the heterobimetallic nature of the complex. However, it resembles the binding interaction in the unsymmetrical donor–acceptor-type Me-bridged [$Cu(PPh_3)_2(\mu$-Me)CuMe] dicopper complex reported by Steffen and co-workers that is also stabilized by metal–metal interactions.[23]

Compared to **3**, NBO analysis shows that complex **4** exhibits only moderate donation from a Pt–Me_A fragment to Cu [$E^{(2)}$ = 44.23 kcal mol^{-1}] and similar metal–metal interactions manifest in the donation from a d-type orbital on Pt to an s-orbital of Cu [$E^{(2)} = 32.13$ kcal mol^{-1}] (Table S13 and Fig. S155†). Weaker donation from the Pt–Me_B fragment to Cu is also observed [$E^{(2)}$ = 17.5 kcal mol^{-1}]. The NBI between the carbon of the distal Me_A and Cu is 0.1985 in **4**, significantly less than in **3**, while NBI between the Pt and Cu centers remain similar (0.2498) (Table S14†).

The detailed analysis of orbital contributions to the Pt→Cu interaction in complexes **3** and **4** shows that the donation from Pt occurs predominantly from the filled d_{z^2}-type orbital in both complexes. This is also consistent with the general description of the dative Pt→Cu bonding in heterobimetallic Pt/Cu complexes reported by Chen and co-workers.[13]

Reactivity of Pt^{II}/Cu^{I} complexes and comparison with monometallic Pt complexes

We first studied the solution-state stability of complexes **3**[X] compared with their monometallic counterpart **1**. The common decomposition pathway for dimethyl Pt complexes with N,P-donor ligands involves rollover cyclometalation leading to undesired C–H bond activation of the ligand.[24] Heating monometallic complex **1** at 40 °C in THF for 12 h (or 3 days in

benzene) led to the expected cyclometalation to form complex **5** characterized by XRD (Scheme 4a). In contrast, bimetallic complex **3**[BF_4] was considerably more stable towards cyclometalation and remained unchanged upon heating in THF at 40 °C for 12 h. The presence of an electrophilic Cu^I center coordinated by the bridging Me group presumably offers some kinetic resistance to rollover cyclometalation.

Surprisingly, when complex **3**[$B(Ar^F)_4$] was heated in C_6H_6 at 80 °C for 18 h, a new complex **6**[$B(Ar^F)_4$] was obtained in 46% *in situ* yield resulting from an aryl group transfer from a $[B(Ar^F)_4]^-$ counteranion to a Pt center (Scheme 4 and Fig. 4). Under the same conditions, complex **3**[BF_4] mostly decomposed (>80%) after heating in C_6H_6 at 80 °C for 18 h to form a mixture of unidentified products. Although such electron deficient aryl group transfer is known for some electrophilic monometallic complexes (Rh, Au, and Pt)[25] and homobimetallic Cu_2 and Fe_2 complexes,[6h,26] this is the first example of such transmetalation from a tetraarylborate anion by a heterobimetallic complex with a formally neutral Pt center. Aryl group transfer upon treatment with a Lewis-acidic BPh_3 was also observed in Me-bridged homobimetallic Cu_2 complexes.[22] Although the fate of the Me group and B-containing product could not be determined, the less than 50% yield of complex **6**[$B(Ar^F)_4$] likely results from the necessity to sacrifice a $[B(Ar^F)_4]^-$ counteranion for aryl group transfer.[20] Indeed, when the reaction was performed in the presence of 4.5 equiv. of Na[$B(Ar^F)_4$], the *in situ* yield of **6**[$B(Ar^F)_4$] increased to 80%.

The X-ray structure of **6**[$B(Ar^F)_4$] reveals close contacts of a Cu^I center with the *ipso*-carbon of an aryl group (2.098(3) Å) and an adjacent *ortho*-carbon (2.335(3) Å), while the distance between Pt^{II} and Cu^I atoms (2.7745(4) Å) is now longer than the sum of their covalent radii, indicating no metal–metal interactions when compared to **3**[X] and also consistent with the lack of bcp according to AIM analysis (Fig. 3 and Table S4†).

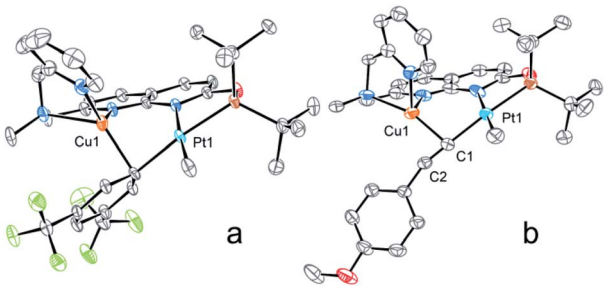

Fig. 4 ORTEP of **6**[$B(Ar^F)_4$] (a) and **7**[BF_4] (b) at the 50% probability level. Hydrogen atoms, counterions, and solvent molecules together with the minor disorder component for **7**[BF_4] are omitted for clarity.

NBO analysis for complex **6**[$B(Ar^F)_4$] reveals strong donation [$E^{(2)} = 62.36$ kcal mol^{-1}] from the Pt–C_{ipso} fragment of Pt–Ar to an empty s-type orbital on Cu (Table S15 and Fig. S157†). Additionally, donation from the p-type orbitals of the π-bond (C_{ipso}=C_{ortho}) to an s-type orbital on Cu is also observed [$E^{(2)} = 27.35$ kcal mol^{-1}], along with the corresponding back-donation from the d-type orbital at Cu to an antibonding π*(C_{ipso}=C_{ortho}) orbital [$E^{(2)} = 15.66$ kcal mol^{-1}]. Compared to **3** and **4**, only moderate donation from a d-type orbital at Pt to an s-orbital at Cu is observed, resulting in a lower NBI between Pt and Cu of 0.2281.

We then examined the reactivity of **3** with a terminal alkyne as this substrate contains a reactive C–H bond and a π-system that can potentially interact with a cationic Cu^I center. The synergistic effect of Cu^I salts has been previously implicated in bimetallic alkyne activation.[4a–c] Importantly, monometallic complex **1** did not show any reaction with 2 equiv. of 4-ethynylanisole at RT for at least 24 h. On the other hand, when **3**[BF_4] was reacted with 2 equiv. of 4-ethynylanisole at RT, acetylide complex **7**[BF_4] was cleanly obtained (Scheme 4). The product was isolated in pure form in 59% yield and fully characterized.

A single crystal XRD study reveals a Pt^{II} center with a σ-bound acetylide ligand, which coordinates to a Cu^I center through the triple bond π-system (Cu1···C1 and Cu1···C2 distances of 1.982(5) Å and 2.141(4) Å). The distance between Pt^{II} and Cu^I is 3.0934(8) Å, indicative of a lack of interaction between two metals after coordination of the Cu center with the carbon atom of acetylide and consistent with AIM analysis (Fig. 3).

NBO analysis also shows strong donation from a Pt–C≡ fragment of Pt-acetylide to an empty s-orbital of Cu [$E^{(2)} = 56.69$ kcal mol^{-1}] (Table S17 and Fig. S159†). Donation from p-type orbitals of a C≡C fragment to Cu [$E^{(2)} = 56.69$ kcal mol^{-1}] and the corresponding back-donation from Cu to an antibonding π*(C≡C) orbital [$E^{(2)} = 16.14$ kcal mol^{-1}] is consistent with a π-coordination of Cu with a triple bond. Only weak donation is observed between a filled d-type orbital at Pt to the empty s-orbital on Cu [$E^{(2)} = 13.38$ kcal mol^{-1}] resulting in a low NBI between the Pt and Cu centers (0.1949).

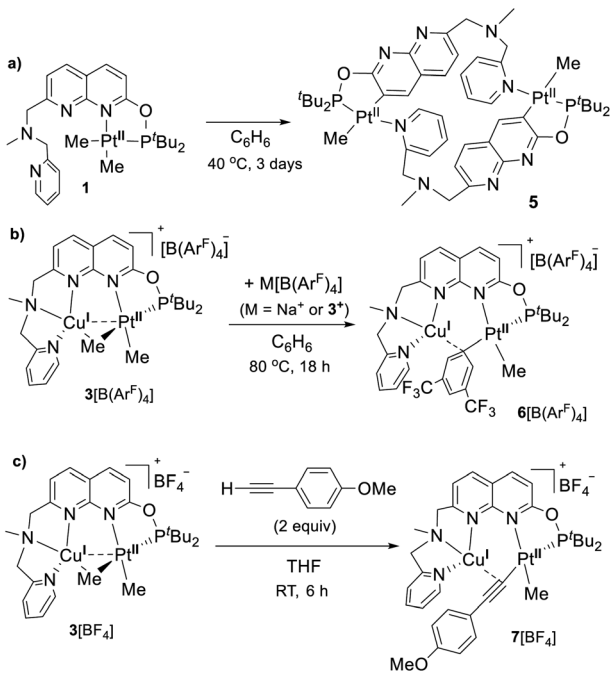

Scheme 4 (a) Cyclometalation of **1**; (b) aryl group transfer from the $[B(Ar^F)_4]^-$ counterion to give **6**; (c) terminal alkyne activation.

The rate constants were measured in a reaction of 3[BF_4] with an excess of phenylacetylene or phenylacetylene-d_1 at −10 °C under pseudo-first order conditions to give the values of $(3.9 \pm 0.2) \times 10^{-4}$ s^{-1} and $(4.4 \pm 0.9) \times 10^{-5}$ s^{-1} for phenylacetylene and phenylacetylene-d_1 labeled at the terminal CH group, respectively. The kinetic isotope effect (KIE) of 9 ± 2 (at −10 °C) suggests that the C–H bond cleavage likely happens at the rate determining step (*vide infra*).[27] The relatively large value for the observed KIE, which is close to the theoretical maximum for the primary KIE, is not uncommon for C–H activation or protonolysis by Pt-methyl complexes[28] and other transition metals.[27] Unusually large values for the KIE (KIE ≥ 7) are often attributed to the tunnelling effect, or in some cases to the geometry of the transition state.[27]

The neutral complex **4** did not show clean reactivity with 2 equiv. of 4-ethynylanisole leading to its eventual decomposition to form multiple products. The lack of well-defined acetylide products is likely due to the significantly higher reactivity of **4** from the presence of a dearomatized ligand arm, which might lead to ligand-centered reactivity, and due to the lack of electrophilicity of the neutral, electron-rich Cu center stabilized by an amide donor.

A computational study of the role of Cu in alkyne activation

Based on the above reactivity, we hypothesize that a cationic Cu^I center plays a role in coordinating the alkyne, thus bringing the substrate in proximity to the Pt center, while increasing the acidity of the terminal C–H bond.[4b] We conducted preliminary DFT studies using a truncated system with propyne as a model substrate and a dimethylphosphinite-substituted ligand, and were able to find an energetically accessible pathway, which involves initial π-coordination of an alkyne with Cu^I of **3′** to initially give π-complex **A** (Fig. 5). NBO calculations reveal enhancement in the polarization of the terminal C–H bond in **A** (charges at C −0.369 and H +0.273) as compared to free propyne (C −0.265 and H +0.239). Oxidative addition to the Pt^{II} center leads to the Pt^{IV} hydride acetylide species **B**, where the triple bond of the alkyne is still π-coordinated to Cu. Due to the weak coordination of the naphthyridine N-donor,[29] low barrier C–H (methane) reductive elimination results in the acetylide complex **C** with a net exergonicity of 28 kcal mol^{-1}.[30] The DFT-calculated KIE for this mechanism is 3.7 at −10 °C (for the truncated system), which is smaller than the observed KIE; however, it is consistent overall with C–H bond activation at the rate determining step.

The alternative concerted protonolysis pathway was also considered, but was found to have a significantly higher barrier of 38.7 kcal mol^{-1}.[30] Because of the use of a truncated system in the preliminary computational analysis, the absolute values should be considered only for qualitative evaluation, and contribution from other possible reaction pathways cannot be excluded.

Although the synergistic effect of Cu^I in terminal alkyne activation is also generally observed in the Sonogashira coupling,[4a–c] the nature of this effect in the case of the Cu^I/Pt^{II} complex described in this work is different and does not involve the transmetalation step, but rather oxidative addition of the C–H to the Pt center. We believe that this is facilitated due to the ability of Cu to act as a "docking site" for an alkyne bringing the C–H bond in proximity to a Pt center and its ability to polarize a C–H bond, making it more prone to further reactivity.

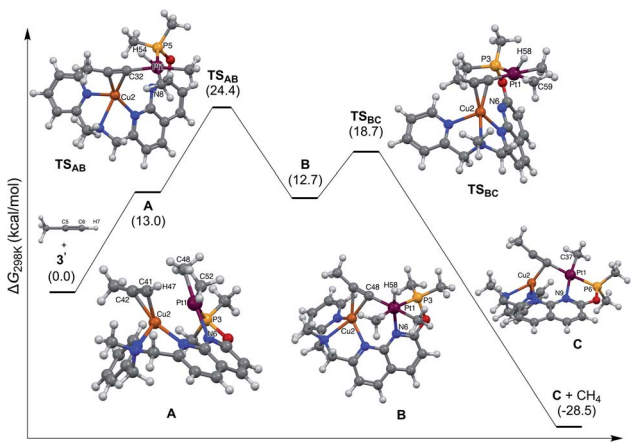

Fig. 5 Calculated energy profile for alkyne activation and DFT-optimized structures for intermediates and transition states.

Conclusions

In summary, we designed and developed a reactive heterobimetallic Pt/Cu species that conclusively demonstrates that proximal interactions with a Cu center alters the reactivity of Pt. We found that a bridging alkyl group between the two metals prevents undesired rollover cyclometalation. The presence of a Cu^I center also induces facile transmetalation from an electron-deficient $[B(Ar^F)_4]^-$ anion and enables facile C–H bond activation of a terminal alkyne. DFT studies elucidate the role of the copper center in coordination and activation of an alkyne substrate which otherwise remains unreactive in the presence of a Pt-only monometallic complex. Considering the increased interest towards the utilization of bimetallic catalysis, this study highlights the principles of ligand design for the study of the metal–metal cooperation effect in organometallic reactivity.

Conflicts of interest

There are no conflicts to declare.

Acknowledgements

O. R.-W. was a JSPS International Research Fellow. This work was supported by JSPS Kakenhi Grant Number 16F16038. The authors thank Mr A. Villar-Briones and Dr M. Roy for performing HR-MS analysis and acknowledge OIST for funding. We thank Dr K. Eguchi (JEOL RESONANCE Inc.) for advice regarding ^{195}Pt NMR.

Notes and references

1 (*a*) P. Buchwalter, J. Rose and P. Braunstein, *Chem. Rev.*, 2015, **115**, 28–126; (*b*) R. C. Cammarota, L. J. Clouston and C. C. Lu, *Coord. Chem. Rev.*, 2017, **334**, 100–111.

2 (*a*) D. R. Pye and N. P. Mankad, *Chem. Sci.*, 2017, **8**, 1705–1718; (*b*) I. G. Powers and C. Uyeda, *ACS Catal.*, 2017, **7**, 936–958.

3 (*a*) N. Yoshikai and E. Nakamura, *J. Am. Chem. Soc.*, 2004, **126**, 12264–12265; (*b*) N. Yoshikai, H. Mashima and E. Nakamura, *J. Am. Chem. Soc.*, 2005, **127**, 17978–17979.

4 (*a*) R. Chinchilla and C. Najera, *Chem. Soc. Rev.*, 2011, **40**, 5084–5121; (*b*) R. Chinchilla and C. Najera, *Chem. Rev.*, 2007, **107**, 874–922; (*c*) M. H. Perez-Temprano, J. A. Casares and P. Espinet, *Chem.–Eur. J.*, 2012, **18**, 1864–1884; (*d*) I. Meana, P. Espinet and A. C. Albéniz, *Organometallics*, 2014, **33**, 1–7; (*e*) R. J. Oeschger, D. H. Ringger and P. Chen, *Organometallics*, 2015, **34**, 3888–3892; (*f*) R. J. Oeschger and P. Chen, *J. Am. Chem. Soc.*, 2017, **139**, 1069–1072.

5 (*a*) V. Farina, S. Kapadia, B. Krishnan, C. Wang and L. S. Liebeskind, *J. Org. Chem.*, 1994, **59**, 5905–5911; (*b*) L. S. Liebeskind and J. Srogl, *J. Am. Chem. Soc.*, 2000, **122**, 11260–11261; (*c*) P. Espinet and A. M. Echavarren, *Angew. Chem., Int. Ed.*, 2004, **43**, 4704–4734; (*d*) J. Z. Deng, D. V. Paone, A. T. Ginnetti, H. Kurihara, S. D. Dreher, S. A. Weissman, S. R. Stauffer and C. S. Burgey, *Org. Lett.*, 2009, **11**, 345–347.

6 (*a*) F. A. Cotton, C. A. Murillo and R. A. Walton, *Multiple Bonds between Metal Atoms*, Springer New York, 2006; (*b*) S. T. Liddle, *Molecular Metal-Metal Bonds: Compounds*, Synthesis, Properties, Wiley, 2015; (*c*) A. L. Gavrilova and B. Bosnich, *Chem. Rev.*, 2004, **104**, 349–383; (*d*) J. K. Bera, N. Sadhukhan and M. Majumdar, *Eur. J. Inorg. Chem.*, 2009, 4023–4038; (*e*) Y.-Y. Zhou and C. Uyeda, *Science*, 2019, **363**, 857–862; (*f*) E. Kounalis, M. Lutz and D. L. J. Broere, *Chem.–Eur. J.*, 2019, **25**, 13280–13284; (*g*) T. C. Davenport and T. D. Tilley, *Angew. Chem., Int. Ed.*, 2011, **50**, 12205–12208; (*h*) M. S. Ziegler, D. S. Levine, K. V. Lakshmi and T. D. Tilley, *J. Am. Chem. Soc.*, 2016, **138**, 6484–6491; (*i*) T. C. Davenport and T. D. Tilley, *Dalton Trans.*, 2015, **44**, 12244–12255.

7 A. Nicolay and T. D. Tilley, *Chem.–Eur. J.*, 2018, **24**, 10329–10333.

8 (*a*) J. P. Krogman and C. M. Thomas, *Chem. Commun.*, 2014, **50**, 5115–5127; (*b*) B. Wu, M. J. T. Wilding, S. Kuppuswamy, M. W. Bezpalko, B. M. Foxman and C. M. Thomas, *Inorg. Chem.*, 2016, **55**, 12137–12148; (*c*) R. J. Eisenhart, L. J. Clouston and C. C. Lu, *Acc. Chem. Res.*, 2015, **48**, 2885–2894; (*d*) P. L. Dunn, R. K. Carlson, L. Gagliardi and I. A. Tonks, *Dalton Trans.*, 2016, **45**, 9892–9901.

9 (*a*) C. Dubs, A. Inagaki and M. Akita, *Chem. Commun.*, 2004, 2760–2761; (*b*) J. Klingele, S. Dechert and F. Meyer, *Coord. Chem. Rev.*, 2009, **253**, 2698–2741; (*c*) M. Konrad, S. Wuthe, F. Meyer and E. Kaifer, *Eur. J. Inorg. Chem.*, 2001, 2233–2240.

10 (*a*) K. M. Engle, T.-S. Mei, M. Wasa and J.-Q. Yu, *Acc. Chem. Res.*, 2012, **45**, 788–802; (*b*) J. He, M. Wasa, K. S. L. Chan, Q. Shao and J.-Q. Yu, *Chem. Rev.*, 2017, **117**, 8754–8786; (*c*) Y.-F. Yang, X. Hong, J.-Q. Yu and K. N. Houk, *Acc. Chem. Res.*, 2017, **50**, 2853–2860.

11 M.-E. Moret, D. Serra, A. Bach and P. Chen, *Angew. Chem., Int. Ed.*, 2010, **49**, 2873–2877.

12 O. Rivada-Wheelaghan, S. L. Aristizábal, J. López-Serrano, R. R. Fayzullin and J. R. Khusnutdinova, *Angew. Chem., Int. Ed.*, 2017, **56**, 16267–16271.

13 M.-E. Moret and P. Chen, *J. Am. Chem. Soc.*, 2009, **131**, 5675–5690.

14 (*a*) E. Fogler, J. A. Garg, P. Hu, G. Leitus, L. J. W. Shimon and D. Milstein, *Chem.–Eur. J.*, 2014, **20**, 15727–15731; (*b*) L. E. Eijsink, S. C. P. Perdriau, J. G. de Vries and E. Otten, *Dalton Trans.*, 2016, **45**, 16033–16039; (*c*) C. A. Huff, J. W. Kampf and M. S. Sanford, *Organometallics*, 2012, **31**, 4643–4645.

15 (*a*) J. R. Khusnutdinova and D. Milstein, *Angew. Chem., Int. Ed.*, 2015, **54**, 12236–12273; (*b*) M. Vogt, O. Rivada-Wheelaghan, M. A. Iron, G. Leitus, Y. Diskin-Posner, L. J. W. Shimon, Y. Ben-David and D. Milstein, *Organometallics*, 2013, **32**, 300–308; (*c*) O. Rivada-Wheelaghan, A. Dauth, G. Leitus, Y. Diskin-Posner and D. Milstein, *Inorg. Chem.*, 2015, **54**, 4526–4538.

16 Deposition numbers 1975187–1975194 contain the supplementary crystallographic data for this paper.†

17 (*a*) L. Yang, D. R. Powell and R. P. Houser, *Dalton Trans.*, 2007, 955–964; (*b*) D. Rosiak, A. Okuniewski and J. Chojnacki, *Polyhedron*, 2018, **146**, 35–41; (*c*) A. Okuniewski, D. Rosiak, J. Chojnacki and B. Becker, *Polyhedron*, 2015, **90**, 47–57.

18 B. Cordero, V. Gomez, A. E. Platero-Prats, M. Reves, J. Echeverria, E. Cremades, F. Barragan and S. Alvarez, *Dalton Trans.*, 2008, 2832–2838.

19 J. Campos, J. López-Serrano, R. Peloso and E. Carmona, *Chem.–Eur. J.*, 2016, **22**, 6432–6457.

20 (*a*) E. G. Hope, W. Levason and N. A. Powell, *Inorg. Chim. Acta*, 1986, **115**, 187–192; (*b*) A. Knodler, W. Kaim, V. K. Jain and S. Zalis, *J. Organomet. Chem.*, 2002, **655**, 218–226; (*c*) J. R. L. Priqueler, I. S. Butler and F. D. Rochon, *Appl. Spectrosc. Rev.*, 2006, **41**, 185–226.

21 (*a*) C. Lepetit, P. Fau, K. Fajerwerg, M. L. Kahn and B. Silvi, *Coord. Chem. Rev.*, 2017, **345**, 150–181; (*b*) L. J. Farrugia, P. R. Mallinson and B. Stewart, *Acta Crystallogr., Sect. B: Struct. Sci.*, 2003, **59**, 234–247; (*c*) G. Gervasio, R. Bianchi and D. Marabello, *Chem. Phys. Lett.*, 2004, **387**, 481–484.

22 M. S. Ziegler, N. A. Torquato, D. S. Levine, A. Nicolay, H. Celik and T. D. Tilley, *Organometallics*, 2018, **37**, 2807–2823.

23 R. Molteni, R. Bertermann, K. Edkins and A. Steffen, *Chem. Commun.*, 2016, **52**, 5019–5022.

24 (*a*) M. L. Scheuermann, K. A. Grice, M. J. Ruppel, M. Rosello-Merino, W. Kaminsky and K. I. Goldberg, *Dalton Trans.*, 2014, **43**, 12018–12025; (*b*) B. Butschke and H. Schwarz, *Chem. Sci.*, 2012, **3**, 308–326.

25 (*a*) H. Salem, L. J. W. Shimon, G. Leitus, L. Weiner and D. Milstein, *Organometallics*, 2008, **27**, 2293–2299; (*b*) S. G. Weber, D. Zahner, F. Rominger and B. F. Straub, *Chem. Commun.*, 2012, **48**, 11325–11327; (*c*) W. V. Konze, B. L. Scott and G. J. Kubas, *Chem. Commun.*, 1999, 1807–1808; (*d*) E. Khaskin, P. Y. Zavalij and A. N. Vedernikov, *J. Am. Chem. Soc.*, 2008, **130**, 10088–10089.

26 S. L. Matthews and D. M. Heinekey, *Inorg. Chem.*, 2011, **50**, 7925–7927.

27 M. Gómez-Gallego and M. A. Sierra, *Chem. Rev.*, 2011, **111**, 4857–4963.

28 (*a*) J. E. Bercaw, G. S. Chen, J. A. Labinger and B.-L. Lin, *Organometallics*, 2010, **29**, 4354–4359; (*b*) B. J. Wik, M. Lersch, A. Krivokapic and M. Tilset, *J. Am. Chem. Soc.*, 2006, **128**, 2682–2696.

29 (*a*) D. M. Crumpton and K. I. Goldberg, *J. Am. Chem. Soc.*, 2000, **122**, 962–963; (*b*) A. T. Luedtke and K. I. Goldberg, *Inorg. Chem.*, 2007, **46**, 8496–8498.

30 See the ESI.†

